Bioorganic & Medicinal Chemistry Letters 19 (2009) 1508–1511

Contents lists available at ScienceDirect

Bioorganic & Medicinal Chemistry Letters

journal homepage: www.elsevier.com/locate/bmcl

Aminofurazans as potent inhibitors of AKT kinase

Meagan B. Rouse [a,*], Mark A. Seefeld [a], Jack D. Leber [a], Kenneth C. McNulty [a], Lihui Sun [a], William H. Miller [a], ShuYun Zhang [b], Elisabeth A. Minthorn [c], Nestor O. Concha [d], Anthony E. Choudhry [e], Michael D. Schaber [e], Dirk A. Heerding [a]

[a] Oncology Chemistry, GlaxoSmithKline, Collegeville, PA 19426, USA
[b] Oncology Biology, GlaxoSmithKline, Collegeville, PA 19426, USA
[c] Drug Metabolism and Pharmacokinetics, GlaxoSmithKline, Collegeville, PA 19426, USA
[d] Computational and Structural Chemistry, GlaxoSmithKline, Collegeville, PA 19426, USA
[e] Enzymology and Mechanistic Pharmacology, GlaxoSmithKline, Collegeville, PA 19426, USA

ARTICLE INFO

Article history:
Received 11 November 2008
Revised 26 December 2008
Accepted 6 January 2009
Available online 9 January 2009

Keywords:
AKT
PKB
Kinase inhibitor
Serine/threonine kinase

ABSTRACT

AKT inhibitors containing an imidazopyridine aminofurazan scaffold have been optimized. We have previously disclosed identification of the AKT inhibitor GSK690693, which has been evaluated in clinical trials in cancer patients. Herein we describe recent efforts focusing on investigating a distinct region of this scaffold that have afforded compounds (**30** and **32**) with comparable activity profiles to that of GSK690693.

Activation of AKT is mediated by tyrosine kinase receptors and phosphoinositide 3-kinase (PI3K) which recruit AKT to the plasma membrane.[1] Subsequent phosphorylation of the two regulatory sites (ser473/thr308) generates the active enzyme, which serves to phosphorylate various downstream proteins.[2] As such, AKT plays a vital role in cell growth, differentiation, and division and is activated in many human tumors; including prostate, breast, and ovarian.[3,4] Therefore, inhibition of the AKT signaling pathway offers an attractive strategy for oncology therapy.

We recently described the lead optimization effort around the aminofurazan series of inhibitors which led to the identification of GSK690693, a compound that has been evaluated as an intravenous (iv) agent in clinical trials (Fig. 1).[5] This effort focused primarily on optimizing the back pocket (C-4) and amino ether side chain (C-7) substitution. In the follow-up effort, we were interested in exploring distinct areas of the scaffold to obtain compounds with improved pharmacokinetic or pharmacodynamic properties to that of GSK690693. The present communication describes our efforts focused on the C-6 side chain series of analogs.

The synthetic route to the C-6 position analogs is illustrated in Scheme 1. Nucleophilic substitution onto nitropyridine **2** regioselectively afforded nitrophenol **3**.[6] Treatment with excess phosphorus oxybromide generated the dibromo pyridine **4** which underwent selective amination to afford ethyl aminopyridine **5**. Exposure to $SnCl_2$ reduced the nitro group while incorporating a chlorine adjacent to the pyridine nitrogen in **6**.[7] The imidazole ring in intermediate **8** was established through an EDC-mediated coupling with cyanoacetic acid followed by cyclodehydration under acid conditions. Installation of the aminofurazan in compound **9** was realized through a two step procedure involving oxime formation followed by cyclodehydration.[5,8,9]

We reasoned that a 6-position side chain could interact with the same Glu 236 residue that was identified in the corresponding 7-position series (see Fig. 2b).[5] Alternatively, this side chain may associate with distinct neighboring residues, such as Asp293 or Asn280. To ascertain the preferred binding mode, we investigated side chains containing both carbon and oxygen linkages. Bromopyridine **9** served as the common intermediate for this series of

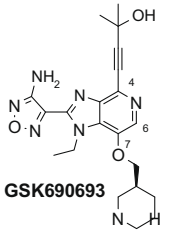

GSK690693

Figure 1. Aminofurazan AKT inhibitor evaluated in clinical trials.

* Corresponding author. Tel.: +1 610 917 7941.
E-mail address: meagan.b.rouse@gsk.com (M.B. Rouse).

0960-894X/$ - see front matter © 2009 Elsevier Ltd. All rights reserved.
doi:10.1016/j.bmcl.2009.01.002

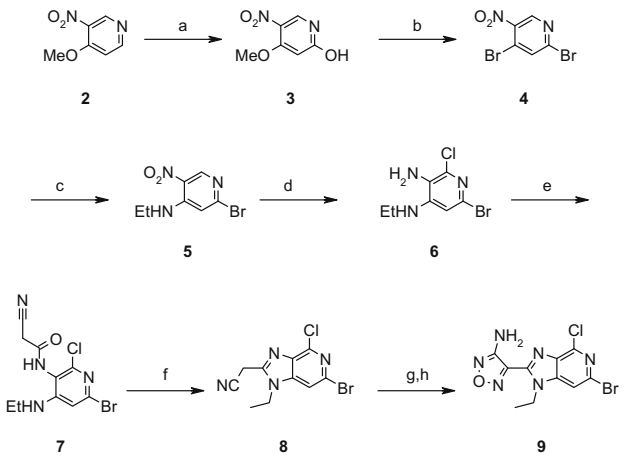

Scheme 1. Reagents and conditions: (a) KO^{t}Bu, ^{t}BuOOH, NH_3, THF, 70%; (b) $POBr_3$, MeCN, 66%; (c) $EtNH_2$, MeOH, THF, 95%; (d) $SnCl_2$, HCl, 60%; (e) cyanoacetic acid, EDC, NMM, DMF, quant.; (f) AcOH, 100 °C; (g) $NaNO_2$, AcOH, 85%; (h) NH_2OH, Et_3N, H_2O, 51%.

analogs (Scheme 2). Regioselective vinylation followed by reductive ozonolysis and Mitsunobu displacement generated the aminomethyl side chain present in intermediate **10**.[10] Intermediate **11**, containing terminal amine substitution, arose from vinylation, ozonolysis, and reductive amination. The extended side chains contained in intermediate **12** were prepared via hydroboration using an appropriate vinyl species followed by in situ Suzuki coupling.[11] The ether linked side chains leading to intermediate **13** were constructed using an optimized two step procedure. First, the aryl boronate derived from lithium-halide exchange in the presence of trimethyl borate was oxidized to give the corresponding pyridone. Subsequent Mitsunobu displacement with a variety of amino alcohols afforded intermediate **13**.[10]

Scheme 3 depicts the remaining transformations to the final analogs **14**–**33**. The alkyne moiety was introduced via a standard Sonogashira coupling.[12] While additional back pocket substitution was explored, the gem-dimethyl alkynol generated the most ideal activity/selectivity profile.[13] Removal of the protecting group from the pendant amine was affected using hydrazine in the case of phthalimide protection or either HCl or TFA in the case of the Boc carbamate.

Table 1 highlights the enzyme and cellular activities for the C-6 substituted aminofurazan analogs. The mechanism based cellular assay evaluated the ability of these compounds to inhibit the phosphorylation of GSK3β, a downstream target of AKT (BT474 cell

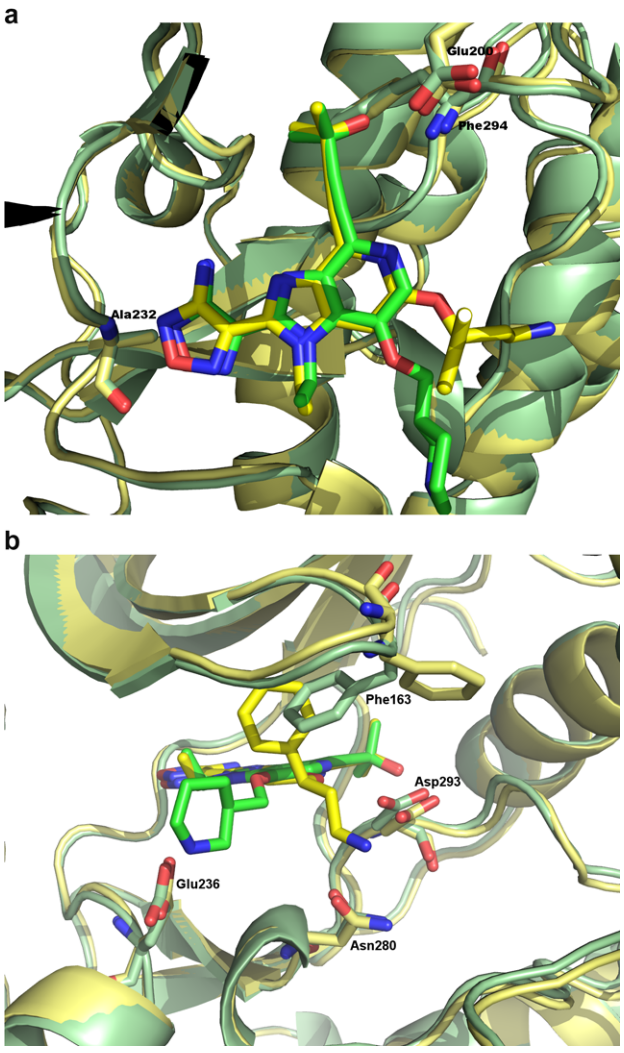

Figure 2. (a) Hinge and back pocket binding modes of **32** (yellow) and GSK690693 (green) in AKT2(148–481).[18] (b) Comparison of the side chain binding modes of **32** (yellow) and GSK690693 (green) in AKT2(148–481).[18]

line). Inhibition of proliferation was measured in both tumor cell lines (BT474 and LNCaP) and non-tumor cells (HFF).[14] For the carbon linked series (entries **14**–**19**), the aminomethyl side chain in compound **14** provided the highest level of cellular potency when compared to the longer chain lengths (**15** and **16**). Additionally,

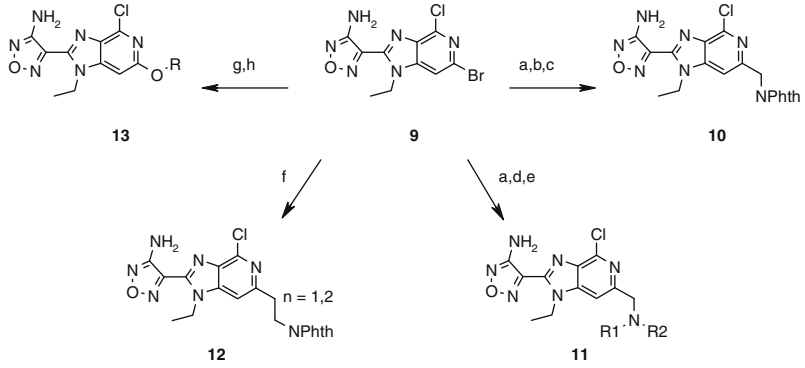

Scheme 2. Reagents and conditions: (a) $Pd(PPh_3)_4$, triethenylboroxin, K_2CO_3, dioxane–H_2O, 75 °C, quant.; (b) Ozone then $NaBH_4$, −78 to 0 °C, 50%; (c) phthalimide, PPh_3, DEAD, THF, 25 °C, 75%; (d) Ozone, −78 °C; (e) R1R2NH, $Na(OAc)_3BH$, MeOH 0 °C, 25–40%—two steps; (f) 9-BBN/vinylphthalimide premix then $Pd(OAc)_2$, dppf, K_2CO_3, DMF, 75 °C, 20–35%; (g) i—$B(OMe)_3$, −105 °C then *n*BuLi; ii—H_2O_2, 3 M NaOH, 50%; (h) ROH, PPh_3, DEAD, 25 °C, 30–75%.

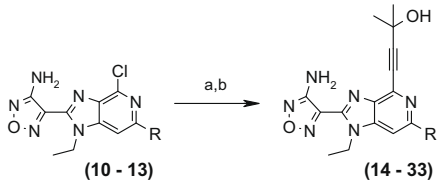

Scheme 3. Reagents and conditions: (a) alkyne, CuI, $Pd(PPh_3)_2Cl_2$, DMF, Et_3N, 80 °C, 50–75%; (b) NH_2Me, MeOH, 45–60% for phthalimide; HCl or TFA, MeOH, 25 °C, 50–70% for Boc.

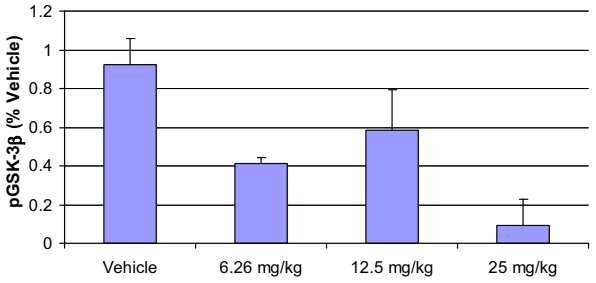

Figure 3. Effect of **30** on GSK3β phosphorylation in BT474 xenografts (ip dosing).

acyclic tertiary amine (**18**) was superior to primary (**14**), secondary (**17**), and cyclic (**19**) amines. Similarly, for the ether linked series (entries **20**–**33**), the aminoethyl chain length (**20**) was more potent than the longer aminopropyl and aminobutyl chain lengths (**21** and **22**). In contrast to the carbon linked series, substitution on the pendant amine was not well tolerated (**23**).

Further exploration revealed that alkyl and aromatic substitution adjacent to the amine offered significant enhancements in enzyme and cellular potency with a clear enantiomeric preference (**24**–**29**).[16] Interestingly, shifting the position of substitution to flank the ether oxygen provided aminoethyl (**30**) and aminopropyl (**32**) compounds with comparable enzyme and cellular profiles to that of GSK690693.

To determine the binding mode for this series, an X-ray co-crystal structure of compound **32** in the kinase domain of AKT2 (148–481) was solved.[17] Figure 2 depicts an overlay of this compound with that of GSK690693. As expected, the binding interactions along the hinge (Ala232) and alkynol (Glu200 and Phe294) residues remained consistent to those previously reported (Fig. 2a).[5] However, the side chain amine showed no apparent binding interactions to the Glu236 resi-

Table 1
SAR for C-6 side chain modifications; compounds **14**–**33**[c,d]

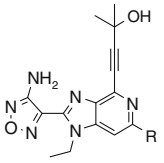

Entry	R	Kinase (IC_{50} nM, [K_i^*])[15]				Cellular activity (IC_{50} nM)			
		Chirality	AKT1	AKT2	AKT3	GSK3β[a]	BT474[b]	LNCaP[b]	HFF[b]
GSK690693	—	—	2 [1]	13 [4]	9	138	69	21	>23,000
14	$-CH_2NH_2$	—	6	63	70	1020	806	296	24,000
15	$-(CH_2)_2NH_2$	—	4	25	NT	4000	1090	2020	24,000
16	$-(CH_2)_3NH_2$	—	3	40	30	13,200	3520	4720	23,000
17	$-CH_2NHCH_3$	—	3	16	NT	303	439	201	5900
18	$-CH_2N(CH_3)_2$	—	2	25	NT	375	357	114	30,000
19		—	6	200	22	2700	1250	313	30,000
20	$-O(CH_2)_2NH_2$	—	5 [6]	40 [39]	43	1140	1080	497	5000
21	$-O(CH_2)_3NH_2$	—	16 [115]	200 [646]	NT	30,000	7120	3180	30,000
22	$-O(CH_2)_4NH_2$	—	63	316	NT	30,000	20,000	6160	30,000
23	$-O(CH_2)_2NHCH_3$	—	12	79	NT	2600	3190	896	17,000
24	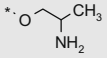	R	8	50	NT	400	860	220	17,000
25		S	13	63	NT	1210	4860	560	28,000
26	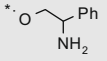	R	3	20	17	1110	2100	124	5000
27		S	5	20	49	1040	3440	176	20,000
28	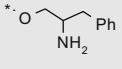	R	0.6 [0.2]	10 [2]	3	80	742	20	8000
29		S	3	20	NT	310	1500	101	7000
30	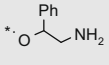	R	1 [0.4]	25 [5]	1	40	35	27	519
31		S	3 [3]	25 [17]	NT	190	124	68	20,000
32	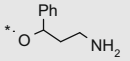	S	2 [0.2]	16 [1]	NT	41	1	5	11,000
33		R	4 [1.9]	50 [105]	65	1570	224	85	29,000

[a] Inhibition of GSK3β phosphorylation (BT474 cells).
[b] Inhibition of proliferation.
[c] Values are the mean of greater than or equal to two experiments.
[d] NT, not tested.

due (Fig. 2b). This amine was instead associated within a unique region of the active site, in the vicinity of Asp293 and Asn280. Additionally, the phenyl ring on the side chain displaced the aromatic ring of the Phe163 residue and engaged in hydrophobic interactions along the glycine rich loop. This may explain the observed enantiomeric preference where the aryl group of the antipode would not be properly oriented to participate in the stacking interaction.

The pharmacokinetics of a representative collection of compounds from this series were examined (**18**, **28**, **30**, and **32**). These compounds displayed PK profiles suitable for iv dosing, similar to that of GSK690693 (data not shown). Unfortunately, there was no evidence of exposure that would allow for oral administration. A representative compound (**30**) was further profiled in a mouse pharmacodynamic study to evaluate the in vivo potency toward inhibition of GSK3β phosphorylation in BT474 xenografts (Fig. 3). This compound showed statistically significant dose dependent inhibition, comparable to the response observed for GSK690693 (data not shown).[5]

In summary, lead optimization around the C-6 position of the aminofurazan template provided analogs with similar enzyme and cellular activity profiles to GSK690693. Additionally, a representative compound displayed an acceptable dose dependent PD response in BT474 tumor xenografts. This series also exhibited a unique binding mode around the amine side chain within the ATP binding pocket. However, there were no improvements in the pharmacokinetic profile which would allow for oral administration. Development of a series with suitable oral properties is underway and will be reported in due course.

Acknowledgments

The authors thank Dr. Melissa Dumble for helpful discussions around in vivo biology and Dr. Kristin Koretke for assistance with molecular modeling.

Supplementary data

Supplementary data associated with this article can be found, in the online version, at doi:10.1016/j.bmcl.2009.01.002.

References and notes

1. Sale, E. M.; Sale, G. J. *Cell. Mol. Life Sci.* **2008**, *65*, 113.
2. Carnero, A.; Blanco-Aparicio, C.; Renner, O.; Link, W.; Leal, J. F. M. *Curr. Cancer Drug Targets* **2008**, *8*, 187.
3. Bellacosa, A.; Kumar, C. C.; Di Cristofano, A.; Testa, J. R. *Adv. Cancer Res.* **2005**, *94*, 29.
4. (a) Lindsley, C. W.; Barnett, S. F.; Layton, M. E.; Bilodeau, M. T. *Curr. Cancer Drug Targets* **2008**, *8*, 7; (b) Li, Q. *Expert Opin. Ther. Patents* **2007**, *17*, 1077.
5. Heerding, D. A.; Rhodes, N.; Leber, J. D.; Choudhry, A. E.; Clark, T. J.; Concha, N. O.; Duckett, D.; Eberwein, D.; Geske, R. S.; Gilmer, T. M.; Huang, P. S.; Kahana, J. A.; Keenan, R. M.; Kleymenova, E. V.; Knick, V. B.; Lafrance, L. V.; Lai, Z.; Lansing, T. J.; Li, M.; McConnell, R. T.; Minthorn, E. A.; Robell, K. A.; Rusnak, D. W.; Safonov, I. G.; Strum, S. L.; Takata, D. T.; Venslavsky, J. W.; Wood, E. R.; Yamashita, D. S.; Zhang, S.; Kumar, R. *J. Med. Chem.* **2008**, *51*, 5663.
6. Makosza, M.; Sienkiewicz, K. *J. Org. Chem.* **1998**, *63*, 4199.
7. Irani, R. J.; SantaLucia, J., Jr. *Nucleosides Nucleotides Nucleic Acids* **2002**, *21*, 737.
8. Bamford, M. J.; Alberti, M. J.; Bailey, N.; Davies, S.; Dean, D. K.; Gaiba, A.; Garland, S.; Harling, J. D.; Jung, D. K.; Panchal, T. A.; Parr, C. A.; Steadman, J. G.; Takle, A. K.; Townsend, T.; Wilson, D. M.; Witherington, J. *Bioorg. Med. Chem. Lett.* **2005**, *15*, 3402.
9. Stavenger, R. A.; Cui, H.; Dowdell, S. E.; Franz, R. G.; Gaitanopoulos, D. E.; Goodman, K. B.; Hilfiker, M. A.; Ivy, R. L.; Leber, J. D.; Marino, J. P.; Oh, H.-J.; Viet, A. Q.; Xu, W.; Ye, G.; Zhang, D.; Zhao, Y.; Jolivette, L. J.; Head, M. S.; Semus, S. F.; Elkins, P. E.; Kirkpatrick, R. B.; Dul, E.; Khandekar, S. S.; Yi, T.; Jung, D. K.; Wright, L. L.; Smith, G. K.; Behm, D. J.; Doe, C. P.; Bentley, R.; Chen, Z. X.; Hu, E.; Lee, D. *J. Med. Chem.* **2007**, *50*, 2.
10. For a review on recent advances in the Mitsunobu reaction see: (a) Dembinski, R. *Eur. J. Org. Chem.* **2004**, *13*, 2763. and references cited therein; (b) Mitsunobu, O.; Wada, M.; Sano, T. *J. Am. Chem. Soc.* **1972**, *94*, 679.
11. (a) Miyaura, N.; Ishiyamo, T.; Ishikawa, M.; Suzuki, A. *Tetrahedron Lett.* **1986**, *27*, 6369; (b) Modrakowski, C.; Camacho Flores, S.; Beinhoff, M.; Schlüter, A. D. *Synthesis* **2001**, *14*, 2143.
12. For a recent review on the Sonogashira coupling reaction see: (a) Chinchilla, R.; Nájera, C. *Chem. Rev.* **2007**, *107*, 874. and references cited therein; (b) Sonogashira, K. *J. Organomet. Chem.* **2002**, *653*, 46.
13. Similar trends in kinase selectivity were observed to those previously reported on this scaffold (see Ref. 5).
14. For a detailed description of the assay methods see Ref. 5.
15. For compounds which approached the limit of detection in our standard IC_{50} assay, K_i values were determined. For a detailed protocol describing this assay see Ref. 5.
16. The chiral amino ether side chains contained in compounds **24**–**33** were commercially available, obtained through reduction of the corresponding amino acid or acquired from chiral resolution of the racemate.
17. Crystallographic data for compound **32** has been deposited with the RSBC Protein Data Bank, PDB code 3E8D.
18. Graphics generated using Pymol (http://www.pymol.org).